



## Molecular Crystals and Liquid Crystals Incorporating Nonlinear Optics

Publication details, including instructions for authors and  
subscription information:

<http://www.tandfonline.com/loi/gmcl17>

### Phase Diagrams and Solid State NMR Studies of Perhydrotriphenylene- Semifluorinated Hydro- carbon Inclusion Compounds

Giuseppe Di Silvestro <sup>a</sup> , Piero Sozzani <sup>a</sup> & Mario Farina <sup>a</sup>

<sup>a</sup> Dipartimento di Chimica Organica e Industriale, Università di  
Milano, Via Venezian 21, I-20133, Milano, Italy

Version of record first published: 22 Sep 2006.

To cite this article: Giuseppe Di Silvestro , Piero Sozzani & Mario Farina (1990): Phase Diagrams and  
Solid State NMR Studies of Perhydrotriphenylene-Semifluorinated Hydro- carbon Inclusion Compounds,  
Molecular Crystals and Liquid Crystals Incorporating Nonlinear Optics, 187:1, 123-134

To link to this article: <http://dx.doi.org/10.1080/00268949008036035>

PLEASE SCROLL DOWN FOR ARTICLE

Full terms and conditions of use: <http://www.tandfonline.com/page/terms-and-conditions>

This article may be used for research, teaching, and private study purposes. Any  
substantial or systematic reproduction, redistribution, reselling, loan, sub-licensing,  
systematic supply, or distribution in any form to anyone is expressly forbidden.

The publisher does not give any warranty express or implied or make any representation  
that the contents will be complete or accurate or up to date. The accuracy of any  
instructions, formulae, and drug doses should be independently verified with primary  
sources. The publisher shall not be liable for any loss, actions, claims, proceedings,  
demand, or costs or damages whatsoever or howsoever caused arising directly or  
indirectly in connection with or arising out of the use of this material.

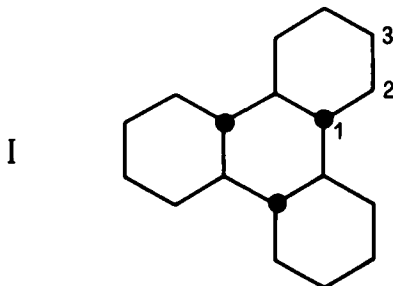
PHASE DIAGRAMS AND SOLID STATE NMR STUDIES  
 OF PERHYDROTRIPHENYLENE-SEMIFLUORINATED HYDROCARBON  
 INCLUSION COMPOUNDS.

GIUSEPPE DI SILVESTRO, PIERO SOZZANI, MARIO FARINA  
 Dipartimento di Chimica Organica e Industriale,  
 Università di Milano, Via Venezian 21, I-20133, Milano, Italy.

**Abstract** The phase diagrams of mixtures of perhydrotriphenylene with linear hydrocarbons, fluorocarbons and semifluorinated compounds forming inclusion compounds, were established by DSC analysis. The results were interpreted within the framework of the regular solution theory. MAS NMR spectroscopy was applied to the inclusion compounds, giving a description of the mobility of the guests in the solid state.

INTRODUCTION

Some years ago we presented a paper concerning the thermodynamic relationships of phase equilibria for binary mixtures forming crystalline adducts.<sup>1</sup> Our interest came from the study of the solid state polymerization of diene monomers included in perhydrotriphenylene (I, PHTP) a crystalline host which easily forms channel-like clathrates with a variety of molecules having different shape, dimension and chemical constitution. After X- or gamma-ray irradiation the crystalline PHTP/monomer inclusion compound is transformed into the PHTP/polymer inclusion compound.



The topochemical nature of the process gives polymers possessing regio- and stereoregularity. Polymerization proceeds in all cases only inside the crystalline adducts.<sup>2</sup>

Due to the coincidence of the P/T range of stability for the inclusion compound with that of the polymerization feasibility, it is of importance to know the complete phase diagram of the system. The PHTP/n-heptane was chosen as a model for the PHTP/monomer inclusion compounds; the phase diagram was determined by tensiometric and calorimetric experiments.<sup>1</sup>

Thermodynamic relationships were proposed under some restrictive hypotheses: immiscibility of the solid phases, ideality in the liquid phase and constancy of the enthalpic parameters with temperature. When host and guest differ in polarizability, deviation from ideality occurs, often reducing the stability of the crystalline adduct. This fact is reflected in the polymerization process, e.g. the highest temperature at which butadiene polymerizes when included in urea is about 100 K lower than that of the corresponding reaction performed in the PHTP adduct.

In a previous communication we accounted for this behavior by using an equation modified according to the theory of regular solutions.<sup>3</sup> In this work we present a comparative study of the phase diagrams of PHTP with some linear molecules with increasing incompatibility with PHTP. We chose as guests n-C<sub>24</sub>H<sub>50</sub> and n-C<sub>24</sub>F<sub>50</sub> and, as cases of intermediate liophobicity, two semifluorinated hydrocarbons differing in the CF<sub>2</sub>/CH<sub>2</sub> ratio.

### EXPERIMENTAL

PHTP was synthesized and purified according to ref. 4. n-C<sub>20</sub>H<sub>42</sub> (H20), n-C<sub>24</sub>H<sub>50</sub> (H24) were chromatographic standards (Farmitalia Carlo Erba, >99.5%, GLC), n-C<sub>20</sub>F<sub>42</sub> (F20) and n-C<sub>24</sub>F<sub>50</sub> (F24) were purchased from Fluka (purity: > 99%, GLC) and used as received.

Semifluorinated hydrocarbons F12H8 and F12H12 were synthesized according to Rabolt<sup>5</sup> from n-C<sub>12</sub>F<sub>25</sub>I and 1-octene or 1-dodecene respectively. Final purification by sublimation gave high purity products (>99.5% GLC).

Pure inclusion compounds of PHTP with H20, H24, F12H8 and F12H12 were obtained from CH<sub>2</sub>Cl<sub>2</sub> solutions.

Mixtures with different composition were directly prepared in the DSC sample holder; DSC analyses were run after melting and slow crystallization in the DSC apparatus. PHTP/F20 or F24 inclusion compounds were obtained by mechanical grinding for 48 h. Lacking direct experimental data concerning fluorinated guests, the host/guest ratio was calculated from that of the corresponding hydrocarbons by adding 0.06 Å for each CF<sub>2</sub>-CF<sub>2</sub> bond to the repeat distance of the hydrocarbon along the channel.<sup>6</sup> DSC apparatus (Mettler TA 3000) was

calibrated with thermometric and calorimetric standards at 1 K/min.

$^{13}\text{C}$  magic angle spinning (MAS) NMR spectra were obtained at 50.3 MHz by a Doty solid state probe operating on a Varian XL-200 instrument with  $\text{Al}_2\text{O}_3$  rotors spinning at 3.5-4 kHz. Cross polarization (CP) was performed after optimizing the Hartmann-Hahn conditions with adamantane. The high power dipolar decoupling (DD) was performed at approximately 10 G. Sweep width: 20 kHz; data points: 8K; number of scans: 1000 - 15000; recycle time: 5s. Spin-lattice relaxation times ( $T_1$ ) were measured on the host signals by the CP  $T_1$  sequence<sup>7</sup> and on the guest signals by using a  $180^\circ$ -tau- $90^\circ$  inversion-recovery pulse sequence with five different tau values ranging from 0.05 to 5 times the  $T_1$  value and a delay of  $5T_1$  between repetitions of the sequence. Chemical shifts were referred to TMS by recording the spectrum of poly(oxymethylene) (POM) before and after each spectrum and taking its signal as being at 89.1 ppm with respect to TMS.

## RESULTS AND DISCUSSION

### Analysis of the phase diagrams

Our system consists of three solid phases, the pure guest (A), host (B) and inclusion compound (C), and of one (L) or two ( $L_1$ ,  $L_2$ ) liquid phases. In cases where a single liquid phase exists, we have to consider three equilibrium curves related to the solubility of the pure A in the liquid phase, the solubility (or decomposition) of clathrate C and the solubility of the host B.

The location of invariant points (eutectic and peritectic) is obtained from the intersection of the curves of corresponding liquid-solid equilibria. For composition other than intersection points, only the curve at higher temperatures for a given composition should be considered in the phase diagram.

By introducing into the theory of regular solutions the approximation of equal molar volumes of A and B, immiscibility of the solid phases, complete dissociation of the adduct in solution and constancy of the melting enthalpy with temperature, the following equations hold true<sup>3,8</sup>:

$$\ln(1-x) + n \ln x = -(\Delta H_C/R)(1/T - 1/T_C) + n \ln n - (n+1) \ln(n+1) - (w/RT)(x^2 + n(1-x)^2 - (n/(n+1))) \quad (1)$$

$$\ln(1-x) = -(\Delta H_A/R)(1/T - 1/T_A) - (w/RT)x^2 \quad (2)$$

$$\ln x = -(\Delta H_B/R)(1/T - 1/T_B) - (w/RT)(1-x)^2 \quad (3)$$

where  $x$  is the molar fraction of the host,  $n$  is the host-guest stoichiometric ratio in the pure inclusion compound,  $\Delta H_C$ ,  $T_C$ ,  $\Delta H_A$ ,  $T_A$ ,  $\Delta H_B$  and  $T_B$  are the melting enthalpy and melting temperature of the inclusion compound (referred to 1 mole of the guest), of the guest and of the host respectively and  $w$  ( $\geq 0$ ) is the repulsive interaction parameter of the regular solution theory.<sup>3</sup> For ideal solutions  $w = 0$  and the Eq. (1-3) are considerably simplified.

Validity of this approach has been verified for several PHTP inclusion compounds.<sup>1,8</sup>

For high  $w$  values the curves derived from Eq. (1-3) are strongly deformed with respect to the ideal ones; in addition, when  $w$  is larger than  $2 RT$ , a miscibility gap is observed in the liquid phase. A new equilibrium curve (the binodal curve) should be taken into account and can be expressed by the following equation<sup>3</sup>:

$$\ln((1-x)/x) = (w/RT)(1-2x) \quad (4)$$

In the presence of the miscibility gap new intersection points are detected in the phase diagram: those between curve (4) and curves (1-3), calculated for the same  $w$  value. The location of invariant points defines the field of stability of the solid phases in the presence of the liquid. In particular the decomposition point of the inclusion compound, in the presence of a miscibility gap with the liquid phase, corresponds to the intersection of curves (2) and (4), provided that both curves (1) and (3) for the same composition lay below such a point.<sup>9</sup>

This approach is successfully applied in the present paper to the decomposition of several binary systems composed by PHTP and a series of hydrocarbons and fluorocarbons.

The first case presented is the PHTP/H<sub>24</sub> system. In Figure 1a)  $T/x$  data are reported; the continuous line corresponds to the Eq. (1) and (2) by using  $T_A = 323.9$  K,  $\Delta H_A/R = 6400$  K,  $T_C = 426.7$ ,  $\Delta H_C/R = 43600$  K,  $w/R = 0$ . PHTP and hydrocarbons show the lowest difference in cohesive energy density and ideality ( $w = 0$ ) should be expected. The good fit between the experimental and calculated values shows any discrepancy from ideality, if existing, to be very low.

Different behavior is observed in PHTP/F<sub>20</sub> or F<sub>24</sub> mixtures; PHTP is immiscible in the liquid phase with perfluorinated molecules even at a temperature as high as 470 K. The Figure 1b) presents the  $T/x$  diagram of the PHTP/F<sub>24</sub> system; a complete immiscibility is observed for any composition. Due to the high melting temperature of the guest, inclusion compound decomposes in the liquid PHTP and in the solid guest. The phase diagram of PHTP/F<sub>20</sub> mixtures is similar except in the  $T_A$  and  $T_C$  values. This behavior corresponds to that predicted by Eq. (1-4) for  $w/R > 2000$  K.

As reported in the Experimental Part, F12H12 and F12H8, like the hydrocarbon analogues, form inclusion compounds with PHTP by

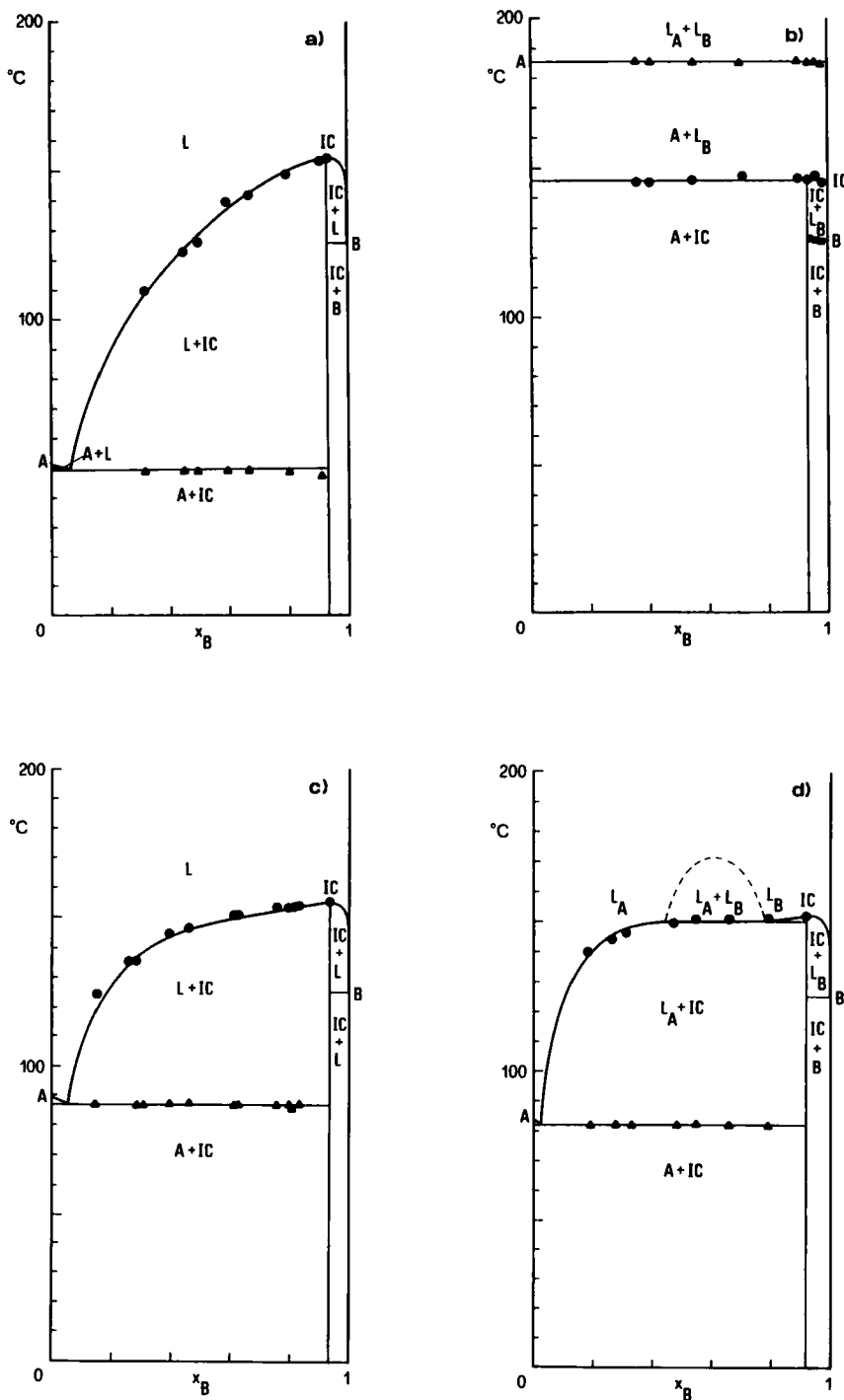


FIGURE 1 Phase Diagrams of PHTP Inclusion Compounds:  
a) PHTP/H24, b) PHTP/F24, c) PHTP/F12H12, d) PHTP/F12H8.

precipitation from  $\text{CH}_2\text{Cl}_2$  solutions. However, strictly controlled conditions are required for the preparation of clathrates from the molten components: their mixtures must be cooled at a rate as low as 1 K/min for obtaining reproducible results. Such behavior is intermediate between PHTP/H24 adduct (obtained at a cooling rate of 5 K/min) and perfluorinated adducts (formed by grinding the two components in the solid state). These facts can be explained by the phase diagram analysis (Table I).

TABLE I The Temperature-composition Data for the PHTP/F12H12 System.  $T_S$  and  $T_L$  are the Solidus and Liquidus Temperatures.

x	$T_S$ (K)	$T_L$ (K)
0.16	360.7	397.5
0.26	360.8	402.1
0.29	360.8	409.3
0.40	360.7	417.6
0.46	360.5	420.4
0.62	360.6	425.2
0.63	359.9	425.2
0.76	360.5	427.1
0.79	360.2	426.3
0.82	359.2	426.5
0.84	360.4	427.4
0.93	-	428.2

The data cannot be interpreted by using Eq. (2) with  $w = 0$  and  $\Delta H_C/R = 43000$  K, as obtained by direct calorimetric measurements; a value of  $w/R = 650$  K, indicating a deviation from ideality, can better fit the data. However, a systematic bias is observed: data obtained at low  $x$  values fall below the curve and those at higher  $x$  are placed above. This bias can be ascribed to the approximations introduced in Eq. (1-3).

Actually, the dependence of  $\Delta H$  and  $w$  on temperature and the difference in molar volume of the components were completely neglected.

Taking into account the difference in specific heat between solid and liquid components, the discrepancy observed at low but not at high  $x$  values - where melting occurs in a limited temperature range - disappears.

As for the second point, several years ago we derived an equation for the solid-liquid equilibrium of an inclusion compound containing a

macromolecular guest, on the basis of the Flory-Huggins theory which takes into account the ratio of molar volumes.<sup>10</sup> Application of this equation however did not substantially improve the fit with experimental data.

A better agreement was obtained by using, for the activity of the components in the liquid phase, equations containing two adjustable parameters. To this purpose we considered the Margules equations expanded to the cubic terms:

$$RT \ln \gamma_G = b x^2 + c x^3 \quad (5)$$

$$RT \ln \gamma_H = (b + 3c/2)(1 - x)^2 - c(1 - x)^3 \quad (6)$$

The best fit was obtained for  $b/R = 280$  K and  $c/R = 470$  K (Figure 1c).

The same equations permit also a description of the PHTP/F12H8 phase diagram. Its behavior differs from the preceding one, approaching that of the perfluorinated guests. A liquid-liquid phase separation occurs after melting in a limited composition range, with a critical temperature estimated around 180 °C. Contrary to expectations derived from equation 4), which is symmetric with respect to composition, the miscibility gap is shifted towards high  $x$  values, as predicted on the basis of equations (5) and (6).

A satisfactory agreement between the calculated solid-liquid curve and the experimental data was obtained by using  $\Delta H_C/R = 37000$  K,  $T_C = 424.7^\circ\text{C}$ ,  $\Delta H_A/R = 3000$  K,  $T_A = 356.5^\circ\text{C}$ ,  $b/R = 360$  K,  $c/R = 350$  K (Figure 1d).

The lack of accurate data about miscibility of semifluorinated hydrocarbons and alkanes in the temperature range allows only a qualitative description of the binodal curve.

#### Magic Angle Spinning NMR Analysis.

Some of the authors have applied solid state NMR techniques in their various forms ( $^{13}\text{C}$  MAS,  $^{13}\text{C}$  and  $^2\text{H}$  broad band) to the study of inclusion compounds formed with high molecular weight molecules.<sup>12-14</sup>

In the present study  $^{13}\text{C}$  Cross Polarized (CP) Magic Angle Spinning (MAS) Dipolar Decoupled (DD) NMR analysis was applied to the adducts of PHTP with C24, F12H12 and F24. In this case we can exploit the presence of independent points of observation: the carbon atoms of the host and those of the guest molecules. The two components behave differently, being endowed with different mobility inside the crystal. Therefore, suitable experiments can be performed in order to evidenciate the host or the guest molecules.

In the CP MAS DD spectra of the inclusion compounds, the PHTP signals at 48, 30 and 26 ppm appear as the main components and are



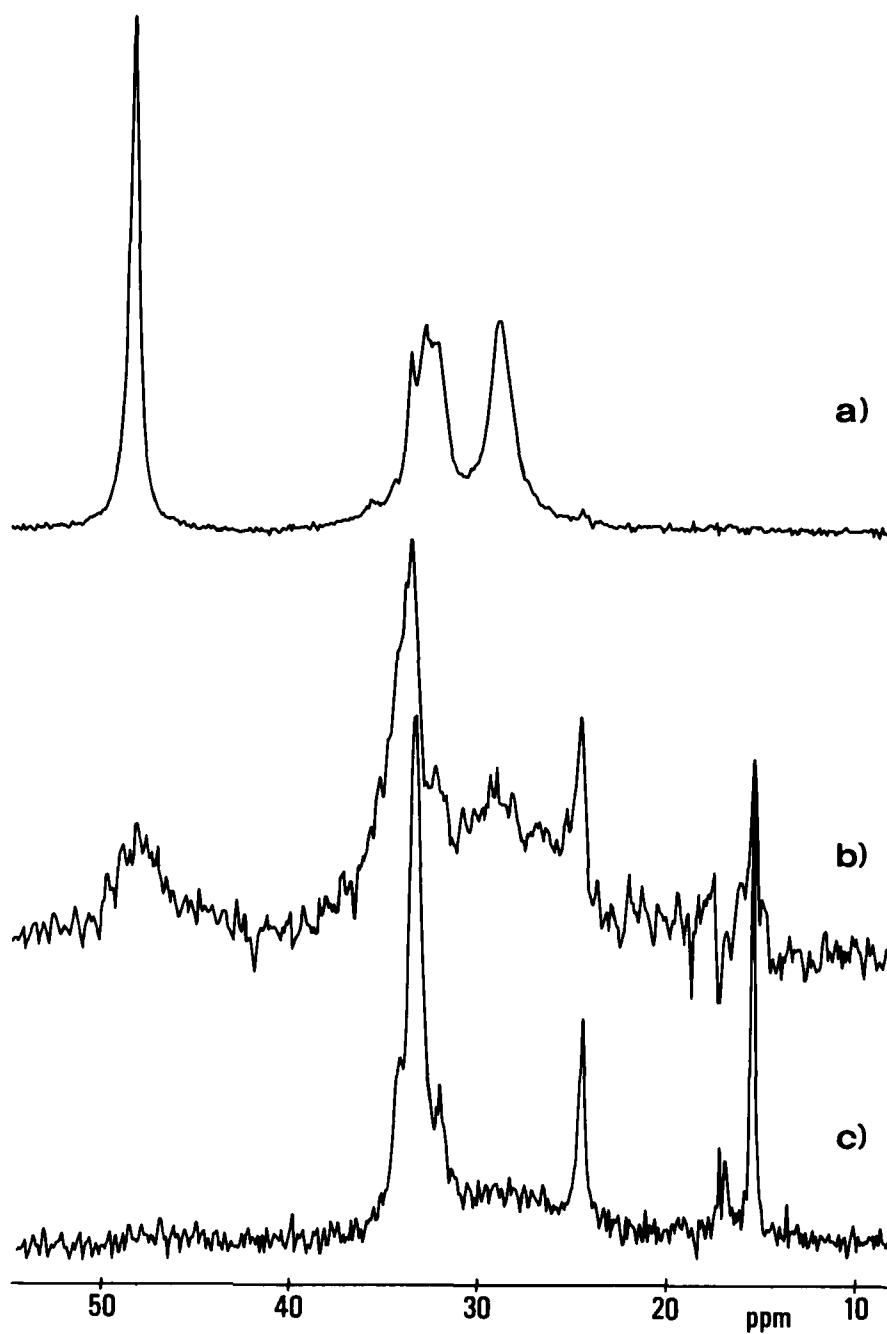


FIGURE 2 High Resolution Solid State  $^{13}\text{C}$  NMR Spectra of PHTP Inclusion Compounds: a) CP MAS DD Spectrum of PHTP/H24, b) MAS DD Spectrum of PHTP/F12H12, c) MAS DD Spectrum of PHTP/H24.

assigned respectively to the carbons 1,2 and 3, in agreement with the solution spectrum. The spectrum of the system PHTP/H24 is reported in Figure 2a, in which the only evidence for the presence of the guest is given by the peak at 33 ppm (internal methylenes of the hydrocarbon chain). The fine splittings of PHTP correspond to those observed in CP MAS spectra of PHTP/polybutadiene, PHTP/polyisoprene and PHTP/low molecular weight compounds, but differ from those of the pure PHTP<sup>14,15</sup>, actually its crystal structure differing from that of the inclusion compound; the NMR pattern appears to be diagnostic of the existence of the latter.<sup>14</sup>

Table II shows the PHTP relaxation times  $T_1$  obtained by the Torchia pulse method<sup>7</sup> for three inclusion compounds with molecules of increasing lyophobicity (C24, F12H12 and F24) compared to the pure PHTP. The overall distribution of the  $T_1$  values is consistent with the crystalline nature of the inclusion compound - the  $T_1$  values are still quite long - but in which PHTP is in a less rigid arrangement than in the pure structure. The  $T_1$  values for the carbons 1 and 2 of the host in the inclusion compounds drop to about one half in comparison to the pure PHTP.

TABLE II Relaxation Times  $T_1$  (s) for the PHTP Carbons in the Inclusion Compounds.

Carbon	1	2	3
PHTP	386	324	258
PHTP/F24	194	199	145
PHTP/H24	165	140	72
PHTP/F12H12	166	141	70, 150

A different behavior is shown by carbon 3 because this carbon is placed towards the channel and is directly sensitive to the interaction with the guest molecules.

This carbon shows longer relaxation times when fluorinated guests are included; semifluorinated guests give intermediate results, showing two components on the exponential decay of PHTP carbon 3, both practically coincident to those of the hydrocarbon and the fluorocarbon inclusion compound. A different mechanism of relaxation could be due to a different polarity of the guest bonds or to a

different mobility and filling of the room available. In spite of the enhanced bulkiness and the better relaxation due to the  $\text{CF}_2$  compared to the  $\text{CH}_2$  groups, the relaxation times are reduced. We suggest therefore that the host-guest interaction is less efficient for fluorocarbons because of a restricted mobility of the guest molecules. This is not surprising if one considers the literature regarding the lower conformational mobility of polytetrafluoroethylene compared with polyethylene.<sup>16</sup>

MAS DD NMR spectra performed without CP are reported in figures 2b and 2c. A short recycle time of 1-5 seconds was chosen in order to suppress by saturation the PHTP signals. This was successfully achieved in the spectrum of PHTP/H24 (Figure 2c). On the other hand the host signals are still present for the system PHTP/F24, although markedly reduced (Figure 2b). By this technique the signals of the hydrocarbons or those of the hydrocarbon moiety of the semifluorinated guest become very clear and well resolved, a demonstration that the spin-lattice relaxation times of the guests do not exceed a few seconds. The carbon atoms of the fluorinated moiety, falling at about 100-120 ppm (not presented), were detected as broad and complicated multiplets due to the fluorine spin, which was not decoupled.

The careful measurements of the relaxation times  $T_1$  confirm the first observations. They are given for PHTP/H24 and the hydrocarbon moiety of PHTP/H12F12, in agreement with a considerable mobility of the chains inside the inclusion compound (13). The chemical shifts of the hydrocarbon moiety are the same for each group in H24 and in H12F12 and are assigned according to the literature<sup>13</sup> (Table III). This portion of the molecules is therefore in the same conformational and motional arrangements both in hydrogenated and in semifluorinated n-alkanes.

TABLE III. Chemical Shifts (ppm) and Relaxation Times (s) of Aliphatic Carbon Atoms of the Guest.

Carbon:	$\text{CH}_3$	alfa	beta	gamma	other
H24	15.2	24.2	33.9	31.8	33.2
F12H12	15.2	24.3	33.7		33.3
$T_1$	3	4			6

The comparison of the absolute values of the chemical shifts with the published MAS NMR data on the n-alkanes in bulk must be drawn carefully, the molecules being in a different environment.<sup>18</sup> The best agreement between the chemical shifts in the bulk and in the inclusion compound (<0.8 ppm) is obtained with the values reported by Moller for the low temperature modification of F12H12.<sup>18</sup> The chemical shifts of the terminal carbon atoms are near those in the melt, while those of the internal methylenes (at 33.1 ppm) fall about 2 ppm downfield with respect to in the melt. This is consistent with the all-trans conformation arrangement along the chain in the inclusion compound. The low values of  $T_1$  relaxation times do not contradict this model because the molecules can undergo an overall rotation around their axis. Similar behavior has already been described in the so called "rotator" phase of many n-alkanes.<sup>19,20</sup>

Note added in proof: This work was ready for printing when a paper was published concerning the solid-liquid diagrams of perfluoro-perfluoro, perfluoro-semifluoro, and fluorocarbon-hydrocarbon mixtures.<sup>21</sup> The reported data are completely consistent with ours and phase diagrams are very well described in terms of equations (2-4).

Acknowledgements. This work was partly supported by grants of CNR (Consiglio Nazionale delle Ricerche), Rome and of the Ministry of Scientific and Technological Research, Rome, Italy. We are indebted to F.A. Bovey and to F.C. Schilling for the use of the NMR instrument at ATT Bell Laboratories, Murray Hill, NJ, USA.

#### REFERENCES

1. M. Farina, G. Di Silvestro, J. Chem. Soc., Perkin Trans. II, 1406 (1980).
2. (a) M. Farina, in Inclusion Compounds edited by J.L. Atwood, J.E.D. Davies, D.D. MacNicol (Academic Press, London, 1984), Vol. 3, Chap. 10, p.297. (b) G. Di Silvestro and P. Sozzani, in Comprehensive Polymer Science edited by G.C. Eastmond, et al. (Pergamon Press, Oxford, 1988), Vol. 4, p. 303.
3. M. Farina, G. Di Silvestro, A. Colombo, Mol. Cryst. Liq. Cryst., **137**, 265 (1986).
4. M. Farina, G. Audisio, Tetrahedron, **26**, 1827 (1970).
5. J.F. Rabolt, T.P. Russel, R.J. Twieg, Macromolecules, **17**, 2786 (1984).

6. G. Allegra, M. Farina, A. Colombo, G. Casagrande Tettamanti, U. Rossi, G. Natta, J. Chem. Soc., B, 1028 (1967).
7. D.A. Torchia, J. Magn. Reson., **30**, 613 (1978).
8. M. Farina, in Inclusion Compounds edited by J.L. Atwood, J.E.D. Davies, D.D. MacNicol (Academic Press, London, 1984), Vol. 2, Chap. 3, p.69.
9. Incidentally we note that equations (2-4) hold true even though components A and B do not form the adduct C.
10. M. Farina, G. Di Silvestro, M. Grassi, Makromol. Chem., **180**, 1041 (1979).
11. J. G. Kirkwood, I. Oppenheim, Chemical Thermodynamics (McGraw-Hill, New York, 1961), p. 176.
12. S. Brückner, P. Sozzani, C. Boeffel, S. Destri, G. Di Silvestro, Macromolecules, **22**, 607 (1989).
13. P. Sozzani, R.W. Behling, F.C. Schilling, S. Brückner, E. Helfand F.A. Bovey, L.W. Jelinsky, Macromolecules, **22**, 3318 (1989).
14. P. Sozzani, F.A. Bovey, F.C. Schilling. Macromolecules, **22**, 4225 (1989).
15. F.C. Schilling, P. Sozzani, F.A. Bovey. ACS Polymer Preprints, **31** n.1 (1990).
16. B.L. Farmer, R.K. Eby, Polymer, **22**, 1487 (1981).
17. (a) D.L. VanderHart, J. Magn. Reson., **44**, 117 (1981). (b) M. Möller, H.J. Cantow, H. Drotloff, D. Emeis, K.S. Lee, G. Wegner, Makromol. Chem., **187**, 1237 (1986).
18. J. Höpken, C. Pugh, W. Richtering, M. Möller, Makromol. Chem., **189** 911 (1988).
19. M.D. Broadhurst, J. Res. Natl. Bur. Stand., **66A**, 241 (1962).
20. G. Zerbi, R. Magni, M. Gussoni, K. Holland-Moritz, A. Bigotto, S. Dirlikov, J. Chem. Phys., **75**, 3175 (1981).
21. D.L. Dorset, Macromolecules, **23**, 894 (1990).